

# A Nonhydrolyzable Reactive cAMP Analogue, (S<sub>p</sub>)-8-[(4-Bromo-2,3-dioxobutyl)thio]adenosine 3',5'-Cyclic S-(Methyl)monophosphorothioate, Irreversibly Inactivates Human Platelet cGMP-Inhibited cAMP Phosphodiesterase at Micromolar Concentrations<sup>†</sup>

Su H. Hung,<sup>‡</sup> K. S. Madhusoodanan,<sup>§</sup> Robert L. Boyd,<sup>‡</sup> James L. Baldwin,<sup>‡</sup> Roberta F. Colman,<sup>§</sup> and Robert W. Colman<sup>\*,‡</sup>

*Thrombosis Research Center, Temple University School of Medicine, Philadelphia, Pennsylvania 19140,  
and Department of Chemistry and Biochemistry, University of Delaware, Newark, Delaware 19716*

*Received October 29, 2001; Revised Manuscript Received December 27, 2001*

**ABSTRACT:** We previously showed that 8-[(4-bromo-2,3-dioxobutyl)thio]adenosine 3',5'-cyclic monophosphate inactivates cAMP phosphodiesterase (PDE3A); however, millimolar concentrations were needed to inactivate PDE3A because of ongoing hydrolysis. We have now synthesized a nonhydrolyzable reactive cAMP analogue, (S<sub>p</sub>)-8-[(4-bromo-2,3-dioxobutyl)thio]adenosine 3',5'-cyclic S-(methyl)monophosphorothioate (S<sub>p</sub>-8-BDB-TcAMPSMe). S<sub>p</sub>-8-BDB-TcAMPSMe inactivates PDE3A in a time-dependent, irreversible manner, exhibiting saturation kinetics with a  $k_{\max}$  of  $(19.5 \pm 0.3) \times 10^{-3} \text{ min}^{-1}$  and a  $K_I$  of  $3.5 \pm 0.3 \text{ } \mu\text{M}$ . To ascertain whether S<sub>p</sub>-8-BDB-TcAMPSMe reacts in the active site, nonhydrolyzable analogues of the substrate cAMP, or the competitive inhibitor cGMP, were included to protect against the inactivation of PDE3A. The order of effectiveness of protectants in decreasing the rate of inactivation (with  $K_d$  values in micromolar) is as follows: S<sub>p</sub>-cAMPS (18) > R<sub>p</sub>-cGMPS (560) and S<sub>p</sub>-cGMPS (1260) > 5'-AMP (17 660), R<sub>p</sub>-cAMPS (30 110), and 5'-GMP (42 170). We docked S<sub>p</sub>-8-BDB-TcAMPSMe into PDE3A, based on the structural model of PDE3A-cAMP and the kinetic data from site-directed mutants. The S<sub>p</sub>-8-BDB-TcAMPSMe fits into the active site in the model. These results suggest that inactivation of PDE3A by the affinity reagent is a consequence of reaction at the overlap between cAMP and cGMP binding regions in the active site. S<sub>p</sub>-8-BDB-TcAMPSMe has proven to be an effective active site-directed irreversible cAMP affinity label for platelet PDE3A and can be used to identify amino acids in the active site of PDE3A as well as in other cAMP phosphodiesterases.

The 11 known families of human cyclic nucleotide phosphodiesterases (PDEs)<sup>1</sup> were characterized on the basis of their sequence homology, substrate specificity, kinetic characteristics, and inhibitor responses as well as physical, regulatory, and immunological properties (1). These enzymes, consisting of 55–60 subtypes, are the products of

25–30 genes with splice and initiation site variations. The catalytic domains of PDEs, comprising the carboxyl-terminal end of the molecules, consist of ~250 conserved amino acids, which are conserved with identities of 30–35% among and 60–65% within families. The regulatory domains of PDEs, comprising the amino-terminal portions, are highly variable among families, which contain sites for phosphorylation, cGMP binding, and membrane insertion.

Intracellular levels of the second messenger cyclic AMP (cAMP) are associated with critical platelet functions such as shape change, aggregation, adhesion, and secretion (2). PDE3A is the most abundant cAMP PDE in platelets, has a low  $K_m$  for cAMP, and is competitively inhibited by cGMP. Nitric oxide (NO) stimulates soluble guanylate cyclase, thereby increasing cGMP levels. Thus, the physiologically important inhibition of platelet functions by NO is probably due to cGMP inhibition of PDE3A, leading to elevated intracellular cAMP levels.

The gene for the catalytic domain of platelet PDE3A from the HEL cell line (3) has been cloned, and the functional protein was produced utilizing a baculovirus-transfected Sf9 insect cell expression system to investigate the active site of PDE3A (4). Site-directed mutagenesis and enzyme kinetic studies have been performed on several highly conserved

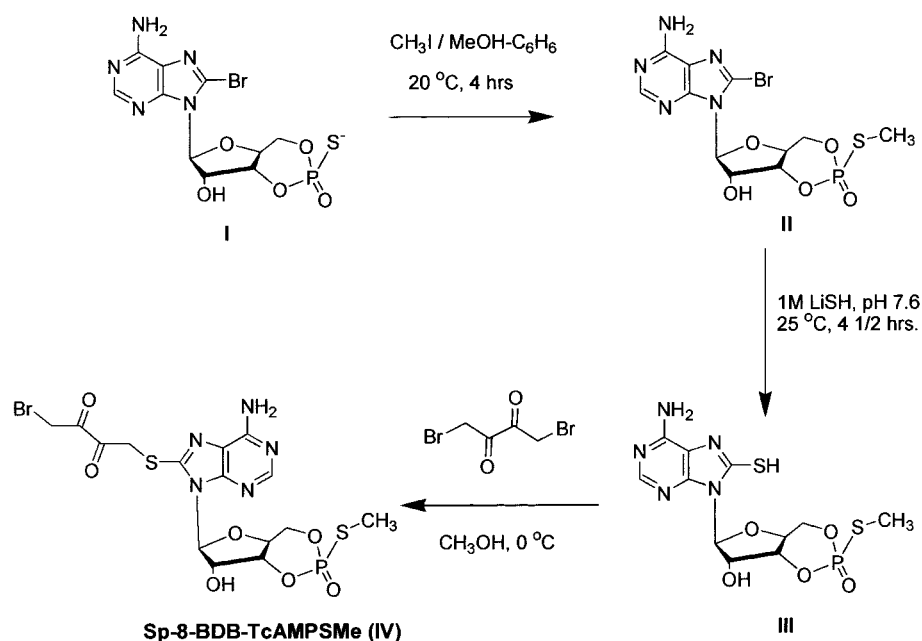
<sup>†</sup> This work is supported by the NSF Grant MCB-97-28202 to R.F.C., NIH Grant HL-64943 to R.W.C., and Training Grant T32 HL07777 to R.W.C. which supported S.H.H. and J.L.B.

\* To whom correspondence should be addressed: Thrombosis Research Center, Temple University School of Medicine, Philadelphia, PA 19140. Phone: (215) 707-4665. Fax: (215) 707-2783. E-mail: colmanr@temple.edu.

<sup>‡</sup> Temple University School of Medicine.

<sup>§</sup> University of Delaware.

<sup>1</sup> Abbreviations: 8-BDB-TcAMP, 8-[(4-bromo-2,3-dioxobutyl)thio]adenosine 3',5'-cyclic monophosphate; S<sub>p</sub>-cAMPS and R<sub>p</sub>-cAMPS, S<sub>p</sub> and R<sub>p</sub> isomers of the nonhydrolyzable adenosine 3',5'-cyclic monophosphorothioate, respectively; S<sub>p</sub>-cAMPS-(BDB), (S<sub>p</sub>)-adenosine 3',5'-cyclic S-(4-bromo-2,3-dioxobutyl)monophosphorothioate; S<sub>p</sub>-8-BDB-TcAMPSMe, (S<sub>p</sub>)-8-[(4-bromo-2,3-dioxobutyl)thio]adenosine 3',5'-cyclic S-(methyl)monophosphorothioate; S<sub>p</sub>-cGMPS and R<sub>p</sub>-cGMPS, S<sub>p</sub> and R<sub>p</sub> isomers of the nonhydrolyzable guanosine 3',5'-cyclic monophosphorothioate, respectively; NO, nitric oxide; PDEs, human cyclic nucleotide phosphodiesterases; cAMP, cyclic AMP; HEL, human erythroleukemia cell line; DBBD, dibromobutanedione; FBS, fetal bovine serum; PIC III, Protease Inhibitor Cocktail set III (100X).

FIGURE 1: Synthesis of  $S_p$ -8-BDB-TcAMPSMe.

amino acids within the active site (3–5). However, this approach cannot elucidate the function of nonconserved amino acids unique to PDE3A.

Affinity labeling using reactive purine nucleotide analogues has been proven to be useful for probing nucleotide binding sites (6–9). We have previously described the use of the cAMP affinity analogue 8-[(4-bromo-2,3-dioxobutyl)-thio]adenosine 3',5'-cyclic monophosphate (8-BDB-TcAMP) in studies to identify amino acids within the active site of PDEs. 8-BDB-TcAMP irreversibly inactivates cAMP-hydrolyzing PDEs and has been used to probe the active site of PDE2A (10), PDE3A (11), and PDE4A (12). In the case of PDE4A, a peptide containing the residue modified by 8-BDB-TcAMP was isolated and the amino acid sequence identified. However, the utility of 8-BDB-TcAMP is limited because it inactivates PDEs only at millimolar concentrations, probably because of continuous hydrolysis to the 5'-AMP derivative by the enzymes that are being investigated.

We have recently demonstrated that  $S_p$ -cAMPS is a potent competitive inhibitor whereas  $R_p$ -cAMPS, like 5'-AMP and 5'-GMP, is a weak inhibitor of PDE3A (13). We now report the synthesis of a new nonhydrolyzable reactive cAMP derivative, ( $S_p$ )-8-[(4-bromo-2,3-dioxobutyl)thio]adenosine 3',5'-cyclic *S*-(methyl)monophosphorothioate ( $S_p$ -8-BDB-TcAMPSMe), which contains both reactive bromoketo and dioxo groups adjacent to the C8 position of the base (Figure 1, compound IV). The bromoketo group can form covalent bonds with the nucleophilic side chains of many amino acids, including cysteine, aspartate, glutamate, histidine, tyrosine, and lysine (7–9, 14), while the dioxo group provides the ability to react with arginine residues (15, 16). We here demonstrate the use of this novel nonhydrolyzable cAMP reagent as an effective affinity label of the catalytic site of PDE3A. A preliminary abstract of this work has been published.<sup>2</sup>

## EXPERIMENTAL PROCEDURES

**Materials.** 1,4-Dibromobutanedione (DBBD), methyl iodide, and trifluoroacetic acid (TFA) were purchased from Aldrich (Milwaukee, WI). 8-Bromo-adenosine 3',5'-cyclic monophosphorothioate,  $S_p$  isomer (Figure 1, compound I), was purchased from Biolog Life Sciences Institute (La Jolla, CA). Lithium hydroxide, HPLC-grade acetonitrile, and methanol were obtained from Fisher Scientific (Pittsburgh, PA). Silica plates (Silica gel 60, 0.2 mm thickness) used for thin-layer chromatography were obtained from E. Merck (Darmstadt, Germany).

Sf9 insect cell lines, the MaxBac Transfection and Expression System, the Xpress Protein Purification System, the NuPage Protein Gel Electrophoresis, Xcell II module, the Chromogenic WesternBreeze System, and Anti-Xpress Antibody were purchased from Invitrogen (Carlsbad, CA). Hink's TNM-FH media and FBS were purchased from Cellgro (Mediatech, Inc., Herndon, VA). PIC III was purchased from Calbiochem (San Diego, CA). Microcon YM-30 centrifugal filter devices were purchased from Millipore (Bedford, MA). Coomassie Plus Protein Assay Reagent Kit and GelCode Blue Stain Reagent were purchased from Pierce (Rockford, IL). Gentamicin sulfate, cAMP,  $S_p$ -cGMPS,  $R_p$ -cGMPS, 5'-AMP, 5'-GMP, and  $\text{NAD}^+$  were purchased from Sigma (St. Louis, MO).  $S_p$ -cAMPS and  $R_p$ -cAMPS used in protection studies were purchased from BIOMOL Research Laboratories, Inc. (Plymouth Meeting, PA). [2,8- $^3\text{H}$ ]Adenosine 3',5'-cyclic phosphate ammonium salt ([2,8- $^3\text{H}$ ]cAMP) was purchased from NEN Life Science Products Inc. (Boston, MA). Biodegradable counting cocktail, Bio-Safe II, was purchased from Research Products International Corp. (Mount Prospect, IL).

**Synthesis of ( $S_p$ )-8-[(4-bromo-2,3-dioxobutyl)thio]adenosine 3',5'-cyclic *S*-(methyl)monophosphorothioate [ $S_p$ -8-BDB-TcAMPSMe (IV)].** Figure 1 shows the scheme for the synthesis of  $S_p$ -8-BDB-TcAMPSMe. Compound IV was synthesized from ( $S_p$ )-8-bromo-adenosine 3',5'-cyclic monophosphorothioate (I) by initial preparation of the more stable

<sup>2</sup> Hung, S. H., Madhusoodanan, K. S., Boyd, R. L., Baldwin, J. L., Colman, R. F., and Colman, R. W. (2001) *Protein Sci.* 10 (Suppl. 2), 93 (A159).

S-methyl derivative (**II**), followed by conversion of the 8-bromo derivative to the 8-mercapto derivative (**III**), and coupling with 1,4-dibromobutanedione to yield the product (**IV**).

(a) *Preparation of (*S*<sub>p</sub>)-8-Bromoadenosine 3',5'-Cyclic S-(Methyl)monophosphorothioate (**II**)*. 8-Bromoadenosine 3',5'-cyclic monophosphorothioate [*S*<sub>p</sub>-8-Br-cAMPS (**I**), 11 mg, 34 μmol] was dissolved in 2 mL of a mixture containing 1 mL each of benzene and methanol. Methyl iodide (8.6 mg, 61 μmol) was added to this solution, and the mixture was stirred at 20 °C for 4 h, at which time the reaction had gone to completion, as indicated by TLC analysis (silica gel plate with a fluorescent indicator, using a 75:10:15 butanol/acetic acid/water solvent system; under these conditions, *S*<sub>p</sub>-8-Br-cAMPS had an *R*<sub>f</sub> value of 0.6 and the product exhibited an *R*<sub>f</sub> value of 0.8). Excess methyl iodide and solvent present in the reaction mixture were removed by rotary vacuum evaporation under reduced pressure to give the pure product (**II**) in 98% yield.

(b) *Preparation of (*S*<sub>p</sub>)-8-Thioadenosine 3',5'-Cyclic S-(Methyl)monophosphorothioate [*S*<sub>p</sub>-8-SH-cAMPSMe (**III**)]*. This reaction was conducted by modification of the procedure reported previously (17, 18). Lithium hydrogen sulfide (1 M LiSH at pH 7.6, 3 mL) was added to a round-bottom flask containing (*S*<sub>p</sub>)-8-bromoadenosine 3',5'-cyclic S-(methyl)monophosphorothioate [*S*<sub>p</sub>-8-Br-cAMPSMe], and the mixture was stirred at 25 °C for 270 min with a steady flow of N<sub>2</sub> gas through the solution. Throughout the course of the reaction, the pH was maintained at 7.6. The reaction's progress was monitored by ultraviolet absorption spectrophotometry. For this purpose, aliquots (typically, 30 μL) of the reaction mixture were withdrawn periodically and diluted with water, and the ultraviolet spectra were recorded. Conversion of *S*<sub>p</sub>-8-Br-cAMPSMe to the 8-thio derivative is accompanied by the decrease in absorbance at 263 nm and increase in absorbance at ~310 nm. After completion of the reaction (~270 min), the mixture was cooled on ice and acidified with acetic acid to pH 6.2. This solution was lyophilized and redissolved in 1 mL of a 0.1% TFA/water mixture. The solution was centrifuged, and the supernatant containing the crude product was subjected to HPLC purification.

A Varian model 5000 HPLC system equipped with a Vydac C<sub>18</sub> analytical column (0.46 cm × 25 cm) was used for the purification of the crude product. The column was equilibrated with 0.1% trifluoroacetic acid in water (0.1% TFA/water, solvent A). After injection of the sample, the column was eluted with solvent A for 15 min followed by a gradient from solvent A to 10% solvent B (0.1% TFA/acetonitrile mixture) over the course of 80 min. A steeper gradient was then run between 10 and 20% solvent B over the course of 60 min, followed by a rapid increase in the amount of solvent B in the eluent from 20 to 100% over the course of 60 min. A constant flow rate of 1 mL/min was maintained throughout the course of the HPLC run. Elution of the product was monitored at A<sub>300</sub>. Under these conditions, the product eluted at 16.8% solvent B. Desired fractions were pooled and lyophilized to obtain the pure product (**III**) in 40% yield.

(c) *Synthesis of (*S*<sub>p</sub>)-8-[(4-Bromo-2,3-dioxobutyl)thio]adenosine 3',5'-Cyclic S-(Methyl)monophosphorothioate [*S*<sub>p</sub>-8-BDB-TcAMPSMe (**IV**)]*. 8-SH-cAMPSMe (3 mg, 10.3

μmol) was dissolved in 250 μL of methanol, and the pH of the solution was adjusted to 5.4 with triethylamine. The solution was quickly mixed with an ice-cold solution of 1,4-dibromobutanedione (40 mg, 164 μmol) in 250 μL of methanol. The solution was vortexed for 3 min, and the volume of the reaction mixture was reduced to 250 μL under a stream of N<sub>2</sub> gas. To this solution was added 13 mL of ice-cold carbon tetrachloride, and the mixture was allowed to stand at 0 °C for 5 min. The precipitated products were collected by centrifugation, washed three times with cold CCl<sub>4</sub> (6 mL each time), and finally dried in a stream of N<sub>2</sub>. The yield was 2.3 mg.

*Analytical Procedures*. The ultraviolet absorption spectra were recorded using a Hewlett-Packard model Vectra XA spectrophotometer, and <sup>31</sup>P NMR spectra were recorded on a Bruker model DRX-400 instrument. The method for determination of the organic phosphorus content of *S*<sub>p</sub>-8-BDB-TcAMPSMe was described previously (19). Briefly, samples containing organic phosphorus were digested prior to analysis by incubating up to 10 nmol of sample (dry or in up to 200 μL) with 20 μL of 10 N H<sub>2</sub>SO<sub>4</sub> at 190 °C for 2 h in a tube closed with aluminum foil. If the residue was colored at this point, 50 μL of 30% H<sub>2</sub>O<sub>2</sub> was added and the sample was incubated again at 190 °C for 1 h in an open tube. A 150–200 μL sample containing inorganic phosphate was mixed with 20 μL of 10 N (NH<sub>3</sub>)<sub>2</sub>SO<sub>4</sub> and 800 μL of a fresh mixture (3:1) of malachite green (0.045% in 0.33 N HCl) and ammonium molybdate (4.2% in 3 N HCl). The A<sub>660</sub> value was measured after 5 min. Determination of the amount of hydrolyzable bromine present in synthetic samples was performed according to a previously reported procedure (19).

*Enzyme Expression and Purification*. Expression of PDE3A using a baculovirus insect cell system and preparation of Sf9 cell lysates have been previously described (4). In short, the DNA fragment encoding the catalytic domain of platelet PDE3A (nucleotides 679–1141) isolated from a HEL cell cDNA library was subcloned into the hexahistidine tag (HIS-tag)-containing baculovirus vector pBlueBacHis2B (pB-BH3031). The PDE3A recombinant virus was produced by cotransfecting Sf9 cells with pBBH3031 and linearized AcMNPV DNA (Invitrogen) using lipofection methods. Sf9 cells grown at 27 °C in Hink's TNM-FH media, containing 10% FBS and 10 μg/mL gentamicin, were infected with the recombinant virus. After 72 h, cells were harvested, mixed with protease inhibitor, and frozen as pellets at –80 °C.

All protein purification procedures were carried out at 4 °C (4). Initially, cell pellets were thawed, suspended in binding buffer [20 mM Na<sub>2</sub>HPO<sub>4</sub>/NaH<sub>2</sub>PO<sub>4</sub>, 0.5 M NaCl, and 20% glycerol (pH 7.8)], retreated with PIC III (10 μL in 1 mL of lysis buffer), and sonicated three times using a sonicator (Heat Systems-Ultrasonics, Inc., Plainview, NY) at output control 5 and a 50% pulsed duty cycle for 1 minute at a time with 30 s rest intervals. Cell debris was removed by centrifugation at 12000g for 20 min using a Sorvall refrigerated centrifuge (SS34 rotor, Dupont, Wilmington, DE). The supernatant was either immediately purified or flash-frozen in liquid nitrogen and stored at –80 °C until further use. HIS-tag PDE3A was isolated using the ProBond nickel resin column contained in the Xpress Protein Purification System. Two milliliters of binding buffer and 2 mL of resin were added to each 1 mL of cell lysate supernatant.



The mixture was rocked for 20 min. The resin–protein complex was washed three times with binding buffer (pH 6.0) and 25 mM imidazole, once with binding buffer (pH 6.5) and 75 mM imidazole, and once with binding buffer (pH 6.7) and 150 mM imidazole to remove non-HIS-tag-containing impurities. The PDE3A was eluted in 10 fractions of 0.5 mL using binding buffer (pH 6.7) and 250 mM imidazole, concentrated, and exchanged into 50 mM Tris-HCl buffer (pH 7.8) containing 10 mM MgCl<sub>2</sub> and 20% glycerol using Microcon YM-30 centrifugal filter devices. Each individual fraction was then assayed for catalytic activity and protein identity using the NuPAGE Protein Gel Electrophoresis System. Active fractions were pooled and stored at –80 °C prior to further characterization.

**Protein Concentration Determination.** The protein concentration was determined with the Coomassie Plus Protein Assay Reagent using bovine serum albumin as the protein standard. The absorbance at 595 nm was measured using a Bio-Tek automatic microplate reader (Bio-Tek Instruments, Inc., Winooski, VT).

**Protein Gel Electrophoresis and Western Blot Analysis of PDE3A.** PDE3A-containing protein solutions and protein standards were subjected to electrophoresis in a 10% Bis-Tris gel with MOPS running buffer using the NuPAGE Protein Gel Electrophoresis System. Gels were either stained with GelCode Blue Stain Reagent or transferred to a PVDF membrane using the Xcell II module at a constant voltage of 25 V for 1 h at room temperature for Western blotting. Transferred membranes were processed using the Chromogenic WesternBreeze System and probed with Anti-Xpress Ab (1:5000 dilution) to detect HIS-tag PDE3A.

**Enzyme Activity Assay.** PDE3A activity was measured as previously described (20). Enzyme-containing solutions were added to buffer containing 50 mM Tris-HCl (pH 7.8), 10 mM MgCl<sub>2</sub>, and 0.8  $\mu$ M [<sup>3</sup>H]cAMP (10 000 cpm/assay) to yield a final volume of 100  $\mu$ L. Reaction mixtures containing experimental samples or no enzyme were incubated at 30 °C for 15 min. The assay was shown to be linear over this time period. Catalysis was terminated by serial addition of 0.2 mL of 0.2 M ZnSO<sub>4</sub> and 0.2 mL of 0.2 M Ba(OH)<sub>2</sub>. Samples were vortexed and centrifuged at 10000g for 5 min. The pellets containing BaSO<sub>4</sub>-precipitated [<sup>3</sup>H]-5'-AMP were discarded. Aliquots of supernatants containing unreacted [<sup>3</sup>H]-cAMP were removed, and counted in a Beckman KS1800 liquid scintillation counter. Enzyme activity was measured by comparing the amount of cAMP hydrolyzed in PDE3A-containing samples to controls without enzyme. These data were then used to calculate enzyme specific activity in nanomoles of cAMP hydrolyzed per milligram of protein per minute.

**Inactivation of PDE3A by S<sub>p</sub>-8-BDB-TcAMPSMe.** Purified PDE3A (152  $\mu$ g/mL) was incubated at 25 °C with S<sub>p</sub>-8-BDB-TcAMPSMe at concentrations of 3.1–100  $\mu$ M in a reaction buffer containing 45 mM HEPES (pH 7.2), 20 mM MgCl<sub>2</sub>, and 4 mM MES. At timed intervals, 5  $\mu$ L aliquots of the reaction mixture were withdrawn, diluted 20-fold in buffer containing 47.5 mM HEPES (pH 7.04), 20 mM MgCl<sub>2</sub>, and 4 mM MES, and assayed in duplicate for residual PDE3A activity. Control samples were incubated under identical conditions except for the absence of S<sub>p</sub>-8-BDB-TcAMPSMe.

**Protection by Ligands against S<sub>p</sub>-8-BDB-TcAMPSMe Inactivation of PDE3A.** The effect of S<sub>p</sub>-cAMPS, R<sub>p</sub>-cAMPS,

S<sub>p</sub>-cGMPS, R<sub>p</sub>-cGMPS, 5'-GMP, 5'-AMP, and NAD<sup>+</sup> on the rate of inactivation of PDE3A were evaluated by incubation of the purified enzyme with each compound for 2 min prior to the addition of S<sub>p</sub>-8-BDB-TcAMPSMe. Aliquots of each final reaction mixture (5  $\mu$ L) were removed at timed intervals, diluted 20-fold in a buffer at 4 °C containing 47.5 mM HEPES (pH 7.04), 20 mM MgCl<sub>2</sub>, and 4 mM MES, and assayed in duplicate for residual PDE3A activity.

**Docking of (S<sub>p</sub>)-Adenosine 3',5'-Cyclic S-(4-Bromo-2,3-dioxobutyl)monophosphorothioate [S<sub>p</sub>-cAMPS-(BDB)] and S<sub>p</sub>-8-BDB-TcAMPSMe to PDE3A.** We used the previously constructed PDE3A-cAMP model (21), which was based on the crystal structure of the catalytic domain of PDE4B (22), as the target for docking the affinity agents, S<sub>p</sub>-cAMPS-(BDB) and S<sub>p</sub>-8-BDB-TcAMPSMe. Briefly, after side chain replacement and loop grafting, the final PDE3A-cAMP structure was subjected to four cycles of dynamics (200 steps) and 50 steps of energy minimization. The minimization was achieved by the conjugate gradient method using the Kollman all-atom force field and Gasteiger–Hückle charges with a dielectric constant of 4 and a nonbonded cutoff of 12 Å. Each of the ligands, S<sub>p</sub>-cAMPS-(BDB) and S<sub>p</sub>-8-BDB-TcAMPSMe, was docked into the PDE3A-cAMP model using Flexidock in the Biopolymer module of the SYBYL Molecular Modeling Environment (Tripos Inc., St. Louis, MO). This program incorporates the van der Waals, electrostatic, torsional, and distance and angle constraint energy terms of the Tripos force field as defined in Sybyl 6.6 (force field manual, p 81). The default conditions of Flexidock differ from those of the Tripos force field only in three respects. The hydrogen van der Waals radius is 1.0 Å; the hydrogen van der Waals  $\epsilon$  is 0.03, and the van der Waals cutoff distance is 16 Å between fragment centroids. The protein is fixed in space, and the ligand is mobile. The flexible side chain bonds of both ligand and protein are adjusted. Only nonring single bonds are rotatable, and backbone atoms are considered fixed. A genetic algorithm is used to determine the optimum ligand geometry. Charges are computed using the Kollman all-atom method for the protein and the Gasteiger–Hückle method for the ligand as defined in Sybyl 6.6 (receptor-based design manual, p 39). First, the active site pocket was defined to consist of amino acid residues (N845, E866, E971, F972, and F100) that exhibited interaction with cAMP from our previous studies (21), which utilized site-directed mutagenesis, enzyme kinetics, and molecular modeling. We next extracted cAMP from the target PDE3A. The water molecules were removed from both S<sub>p</sub>-cAMPS-(BDB) or S<sub>p</sub>-8-BDB-TcAMPSMe and PDE3A. The atom types were checked, and the hydrogen and charge were added. The ligands S<sub>p</sub>-cAMPS-(BDB) and S<sub>p</sub>-8-BDB-TcAMPSMe were prepositioned in the cavity, and the flexible docking between the target and ligand was then performed. The energy of the S<sub>p</sub>-cAMPS-(BDB) or S<sub>p</sub>-8-BDB-TcAMPSMe docking to PDE3A was obtained from the log file after the completion of each docking process. Each of the S<sub>p</sub>-cAMPS-(BDB) and S<sub>p</sub>-8-BDB-TcAMPSMe ligands was docked at least three times to the target enzyme.

## RESULTS

**Characterization of S<sub>p</sub>-8-Br-cAMPSMe, S<sub>p</sub>-8-SH-cAMPSMe, and S<sub>p</sub>-8-BDB-TcAMPSMe.** The ultraviolet absorption spectrum of S<sub>p</sub>-8-Br-cAMPSMe (Figure 1, compound II)

recorded in water at pH 6.4 exhibited a single peak with a  $\lambda_{\max}$  at 263 nm ( $\epsilon = 17\,000\text{ M}^{-1}\text{ cm}^{-1}$ ).  $^{31}\text{P}$  NMR (in  $\text{D}_2\text{O}$ , pH 7.1) analysis revealed a single peak centered at 31.6 ppm as compared to the value of 54.8 ppm exhibited by  $S_p$ -8-Br-cAMPS. This shift is consistent with the alkyl substitution of a phosphorothioate (23–26).

The ultraviolet absorption spectrum of  $S_p$ -8-SH-cAMPSMe (Figure 1, compound **III**) recorded in MES buffer (0.05 M, pH 6.0) exhibited a maximum at 309 nm.  $^{31}\text{P}$  NMR (in  $\text{D}_2\text{O}$ , pH 7.1) analysis exhibits a single peak centered at 31.6 ppm, showing the presence of an unaltered cyclic phosphoro-*S*-methylthioate present in  $S_p$ -8-SH-cAMPSMe.

The ultraviolet absorption spectrum of  $S_p$ -8-BDB-TcAMPSMe (Figure 1, compound **IV**) recorded in MES buffer (0.05 M, pH 6.0) exhibits a single peak with a  $\lambda_{\max}$  of 271 nm [ $\epsilon = 14\,900\text{ M}^{-1}\text{ cm}^{-1}$ , based on the amount of chemically determined organic phosphorus (19) present in the sample]. Determination of the amount of hydrolyzable bromine shows the presence of 1.3 mol of bromine/mol of  $S_p$ -8-BDB-TcAMPSMe. These results are all consistent with the structure of compound **IV** shown in Figure 1.

**Inactivation of PDE3A by  $S_p$ -8-BDB-TcAMPSMe.** To determine whether  $S_p$ -8-BDB-TcAMPSMe inactivates PDE3A, we incubated the enzyme with various concentrations of  $S_p$ -8-BDB-TcAMPSMe from 3.1 to 100  $\mu\text{M}$  for 60 min in 50 mM Hepes buffer (pH 7.5) containing 5 mM  $\text{MgCl}_2$  and 20% glycerol. The inactivation of PDE3A by  $S_p$ -8-BDB-TcAMPSMe is a time-dependent, irreversible reaction (Figure 2A,B). When incubated under the same conditions except for the absence of reagent, PDE3A exhibits constant activity over the course of 60 min at 95% of the residual activity (Figure 2A). The initial rate constant ( $k_{\text{obs}}$ ) of inactivation was determined at each concentration of  $S_p$ -8-BDB-TcAMPSMe that was tested using the equation  $[\ln(y_1) - \ln(y_2)]/(t_1 - t_2)$ , where  $y_1$  is the residual activity ( $E/E_0$ ) measured at time  $t_1$  and  $y_2$  is the residual activity measured at time  $t_2$ . As seen in Figure 2C, the pseudo-first-order rate constant exhibits a nonlinear dependence on the concentration of  $S_p$ -8-BDB-TcAMPSMe. Saturation of the enzyme is achieved at  $S_p$ -8-BDB-TcAMPSMe concentrations of  $>25\text{ }\mu\text{M}$ . This result indicates that there is reversible binding followed by irreversible inactivation. The observed rate constant ( $k_{\text{obs}}$ ) can be described by

$$k_{\text{obs}} = \frac{k_{\text{max}}[R]}{K_1 + [R]}$$

where  $[R]$  is the reagent concentration used for each  $k_{\text{obs}}$ ,  $k_{\text{max}}$  is the maximum rate constant at a saturating concentration of  $S_p$ -8-BDB-TcAMPSMe, and  $K_1 = (k_{-1} + k_{\text{max}})/k_1$ , the apparent dissociation constant of the enzyme–reagent complex. The data shown in Figure 2C were analyzed using Enzfitter (Biosoft, Ferguson, MO). The calculated  $k_{\text{max}}$  equals  $0.0195 \pm 0.0003\text{ min}^{-1}$ , and  $K_1$  equals  $3.5 \pm 0.3\text{ }\mu\text{M}$ .  $S_p$ -8-BDB-TcAMPSMe irreversibly inactivates PDE3A, since no reactivation was observed upon dialysis following the inactivation reaction.

**Effects of Substrate, Inhibitors, and Products on the Rate of Inactivation by  $S_p$ -8-BDB-TcAMPSMe.** To determine whether the reaction occurs within the active site, the ability of various ligands to protect against 25  $\mu\text{M}$   $S_p$ -8-BDB-TcAMPSMe inactivation was tested. To demonstrate protec-

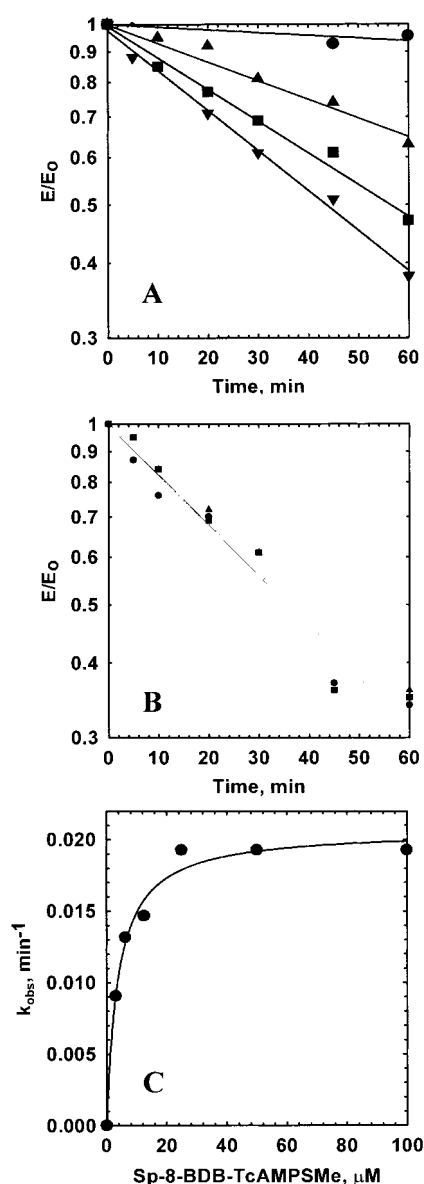


FIGURE 2: Time course of the inactivation of PDE3A by  $S_p$ -8-BDB-TcAMPSMe. The enzyme was incubated at 25  $^{\circ}\text{C}$  with  $S_p$ -8-BDB-TcAMPSMe in 50 mM Hepes buffer (pH 7.5), 20% glycerol, and 5 mM  $\text{MgCl}_2$ . At timed intervals, 5  $\mu\text{L}$  aliquots were removed, diluted 20-fold, and assayed in duplicate for PDE3A catalytic activity. Plot A depicts the average of two experiments utilizing  $S_p$ -8-BDB-TcAMPSMe: ( $\bullet$ ) 0, ( $\blacktriangle$ ) 3.1, ( $\blacksquare$ ) 6.3, and ( $\blacktriangledown$ ) 12.5  $\mu\text{M}$ . Plot B depicts the average of two experiments utilizing  $S_p$ -8-BDB-TcAMPSMe: ( $\bullet$ ) 25, ( $\blacksquare$ ) 50, and ( $\blacktriangle$ ) 100  $\mu\text{M}$ . Plot C depicts the pseudo-first-order rate constant ( $k_{\text{obs}}$ ) for inactivation of PDE3A by  $S_p$ -8-BDB-TcAMPSMe at concentrations ranging from 0 to 100  $\mu\text{M}$ .

tion (if it occurs), we chose a concentration of each ligand equal to or higher than its  $K_i$  value (13) for the protection assay. A nonhydrolyzable substrate analogue,  $S_p$ -cAMPS (45  $\mu\text{M}$ ), protects against inactivation of PDE3A by  $S_p$ -8-BDB-TcAMPSMe, causing a 18.2-fold decrease in pseudo-first-order rate constant [ $k_{\text{obs}} = 0.0010\text{ min}^{-1}$  compared to  $0.0182\text{ min}^{-1}$  with no ligand present (Figure 3A)]. In contrast,  $R_p$ -cAMPS protects against inactivation only at higher concentrations (10 mM) causing an  $\sim 23\%$  decrease in  $k_{\text{obs}}$  (Figure 3B). The concentrations of two nonhydrolyzable cGMP analogues  $S_p$ -cGMPS (750  $\mu\text{M}$ ) and  $R_p$ -cGMPS (750  $\mu\text{M}$ ) were chosen to be high relative to their  $K_i$  values [305 and 210  $\mu\text{M}$ , respectively (13), as seen in Figure 3A].  $S_p$ -cGMPS

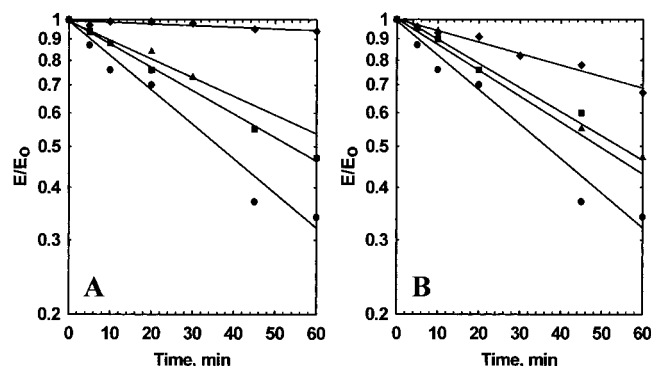


FIGURE 3: Effect of  $S_p$ -cAMPS,  $R_p$ -cAMPS,  $S_p$ -cGMPS,  $R_p$ -cGMPS, 5'-AMP, and 5'-GMP on the inactivation of PDE3A by  $S_p$ -8-BDB-TcAMPSMe. The enzyme was preincubated with various concentrations of protectants for 2 min; 25  $\mu$ M  $S_p$ -8-BDB-TcAMPSMe was added to the reaction mixture, and at time intervals, 5  $\mu$ L aliquots were removed and assayed for PDE3A catalytic activity. Plot A depicts the concentrations of protectants used in the studies: (●) no protectant, (■) 750  $\mu$ M  $S_p$ -cGMPS, (▲) 750  $\mu$ M  $R_p$ -cGMPS, and (◆) 30  $\mu$ M  $S_p$ -cAMPS. Plot B depicts the concentrations of protectants used in the studies: (●) no protectant, (■) 20 mM 5'-GMP, (▲) 10 mM  $R_p$ -cAMPS, and (◆) 25 mM 5'-AMP.

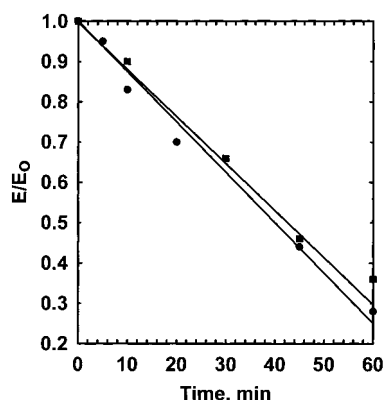


FIGURE 4: Effect of  $NAD^+$  on the inactivation of PDE3A by  $S_p$ -8-BDB-TcAMPSMe. The enzyme was preincubated with  $NAD^+$  for 2 min before 25  $\mu$ M  $S_p$ -8-BDB-TcAMPSMe was added to the reaction mixture. At timed intervals, 5  $\mu$ L aliquots were removed and assayed for PDE3A catalytic activity. The experimental points are as follows: (●) no  $NAD^+$  and (■) 10 mM  $NAD^+$ .

(750  $\mu$ M) and  $R_p$ -cGMPS (750  $\mu$ M) cause a decrease in  $k_{obs}$  to 0.0122 and 0.0101  $\text{min}^{-1}$ , respectively. The product of catalysis, 5'-AMP (25 mM), and the inhibitor metabolite, 5'-GMP (20 mM), protect against inactivation only at much higher concentrations (Figure 3B), and these were in a concentration range higher than their  $K_i$  values [9.6 and 5.6 mM, respectively (13)].  $NAD^+$ , a purine nucleotide that is neither a substrate nor a competitive inhibitor, does not affect the rate of inactivation of PDE3A by  $S_p$ -8-BDB-TcAMPSMe (Figure 4). These results suggest that  $S_p$ -8-BDB-TcAMPSMe targets the active site of the enzyme in the overlap region occupied by both cAMP and cGMP.

**Concentration Dependence of Protectants against Inactivation of PDE3A by 25  $\mu$ M  $S_p$ -8-BDB-TcAMPSMe.** To obtain the apparent dissociation constant ( $K_d$ ) for each protectant, various concentrations of ligands were tested. The apparent dissociation constant for the protectants ( $K_d$ ) was calculated using the equation  $k_{obs} = k_{-ligand}/(1 + [\text{ligand}]/K_d)$ , where  $k_{obs}$  is the pseudo-first-order rate constant at a given ligand concentration,  $k_{-ligand}$  is the rate constant without

Table 1: Apparent  $K_d$  Values of cAMP and cGMP Analogues Measured from Protection against Inactivation by  $S_p$ -8-BDB-TcAMPSMe<sup>a</sup>

cAMP and cGMP analogue	$K_d$ ( $\mu$ M)	$K_i$ ( $\mu$ M)
$S_p$ -cAMPS	$18.3 \pm 1.8$	$47.6 \pm 6.2$
$R_p$ -cAMPS	$30110 \pm 5400$	$4400 \pm 2600$
5'-AMP	$17660 \pm 2110$	$9600 \pm 3060$
$S_p$ -cGMPS	$1260 \pm 260$	$305 \pm 54$
$R_p$ -cGMPS	$560 \pm 350$	$210 \pm 33$
5'-GMP	$42170 \pm 5900$	$5600 \pm 3110$

<sup>a</sup> The  $K_d$  values were calculated using the equation  $k_{obs} = k_{-ligand}/(1 + [\text{ligand}]/K_d)$ . Ligands are the cAMP or cGMP analogues. The  $K_i$  values are cited from ref 13. The  $K_m$  of cAMP is  $0.46 \pm 0.20$   $\mu$ M.

ligand, and  $K_d$  is the apparent dissociation constant for the ligand. Table 1 indicates that  $S_p$ -cAMPS has a smaller  $K_d$  value ( $18.3 \pm 1.8$   $\mu$ M) than  $R_p$ -cAMPS,  $S_p$ -cGMPS, and  $R_p$ -cGMPS ( $30110 \pm 5400$ ,  $1260 \pm 260$ , and  $550 \pm 350$   $\mu$ M, respectively).  $R_p$ -cAMPS, which does not inhibit the enzyme, has a  $K_d$  value which is 1600-fold greater than that of  $S_p$ -cAMPS.  $S_p$ -cAMPS, therefore, is the most effective ligand in protecting PDE3A against inactivation by  $S_p$ -8-BDB-TcAMPSMe.

**Flexidock of  $S_p$ -cAMPS-(BDB) and  $S_p$ -8-BDB-TcAMPSMe into the Active Site of PDE3A.** To decipher the molecular basis of affinity reagents  $S_p$ -8-BDB-TcAMPSMe and  $S_p$ -cAMPS-BDB within the active site of the enzyme, we docked these compounds individually into PDE3A. On the basis of the model of PDE3A-cAMP and kinetic data from site-directed mutants (21, 22), a defined cAMP binding pocket consisting of N845, E866, E971, F972, and F1004 was chosen. Panels A and B of Figure 5 show the models of PDE3A with  $S_p$ -8-BDB-TcAMPSMe and  $S_p$ -cAMPS-BDB docked. The distance between two reacting carbons [C10 for  $S_p$ -8-BDB-TcAMPSMe and C9 for  $S_p$ -cAMPS-(BDB)] is 8.6 Å.

## DISCUSSION

In this paper, we demonstrate that the nonhydrolyzable cAMP analogue  $S_p$ -8-BDB-TcAMPSMe acts as a reactive affinity label, which irreversibly inactivates PDE3A. The kinetic results from the protection against inactivation of PDE3A by the substrate or inhibitor analogues and the position of  $S_p$ -8-BDB-TcAMPSMe in the model suggest that the inactivation of PDE3A results in a reaction at the overlap of both cAMP and cGMP binding regions in the active site.

We have previously shown that the value of  $K_d$  for  $R_p$ -cAMPS is 900-fold larger than that of  $S_p$ -cAMPS in the protection of inactivation by  $S_p$ -cAMPS-(BDB) (13). In this report,  $R_p$ -cAMPS has a  $K_d$  value that is 1600-fold greater than that of  $S_p$ -cAMPS in the protection of inactivation by  $S_p$ -8-BDB-TcAMPSMe. This marked difference in the  $K_d$  values between  $S_p$ -cAMPS and  $R_p$ -cAMPS in the protection of inactivation by both  $S_p$ -cAMPS-(BDB) and  $S_p$ -8-BDB-TcAMPSMe is supported by the results conferred by the docking models of both the  $S_p$ -cAMPS- and  $R_p$ -cAMPS-bound enzymes (13). The difference in the diastereoisomeric centers of  $S_p$ -cAMPS and  $R_p$ -cAMPS has led to a distinct change in their relative orientations in the active site. This difference has positioned  $R_p$ -cAMPS out of the hydrophobic range of F1004 (minimum distance of 7.0 Å).

The nonhydrolyzable cAMP analogue  $S_p$ -8-BDB-TcAMPSMe is as effective as  $S_p$ -cAMPS-(BDB) for the inactivation



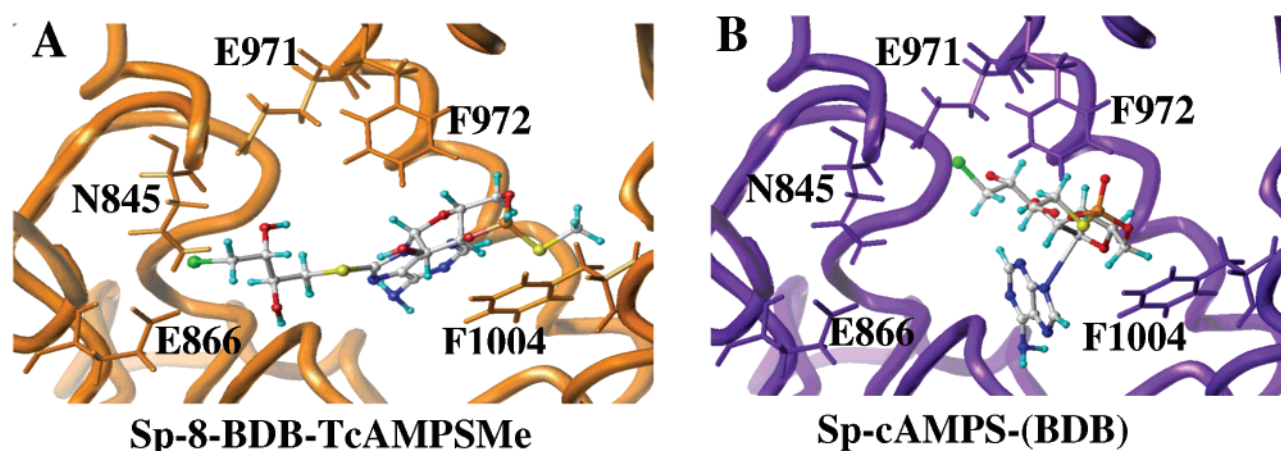


FIGURE 5: Models of  $S_p$ -8-BDB-TcAMPSMe and  $S_p$ -cAMPS-(BDB) docked to PDE3A. Graph A shown in orange depicts the  $S_p$ -8-BDB-TcAMPSMe–enzyme docking model. Graph B shown in purple depicts the  $S_p$ -cAMPS-(BDB)–enzyme docking model. The affinity agents,  $S_p$ -8-BDB-TcAMPSMe and  $S_p$ -cAMPS-(BDB), are shown as ball-and-stick models. The amino acid residues (N845, E866, E971, F972, and F1004) responsible for cAMP binding are shown in capped stick format. The backbone of the PDE3A is shown in tube/ribbon format. The energies between the two compounds,  $S_p$ -8-BDB-TcAMPSMe and  $S_p$ -cAMPS-BDB, docked to the enzyme are  $-23.6 \pm 1.2$  and  $-22.1 \pm 1.5$  kcal/mol, respectively, which are similar to that of  $S_p$ -cAMPS bound to the enzyme ( $-23.5 \pm 1.0$  kcal/mol).

of PDE3A. Micromolar concentrations of  $S_p$ -8-BDB-TcAMPSMe are required to inactivate PDE3A, whereas millimolar concentrations of 8-BDB-TcAMP are needed for enzyme inactivation (10–12). Analogues of the substrate  $S_p$ -cAMPS and inhibitors  $S_p$ -cGMPS and  $R_p$ -cGMPS protect against inactivation of PDE3A by  $S_p$ -8-BDB-TcAMPSMe at micromolar concentrations. These analogues are clearly much more potent than cAMP or cGMP which have to be used at millimolar concentrations to protect against the inactivation of PDE2A, PDE3A, and PDE4A.

Site-directed mutagenesis and enzyme kinetic studies have been performed on several highly conserved amino acids within the active site of PDE3A (4, 5, 21), including the four histidines in metal binding motifs (HNXXH and HDXXH) and their downstream glutamate residues. Kinetic studies of PDE3A mutants have led to a number of conclusions about the functional importance of specific amino acids. It appears that H752 and H756 in the first motif are involved in catalysis, metal binding, or both. Amino acid residue E825, which is downstream and proximate to a unique 44-amino acid insert in PDE3A, appears to interact with cGMP. Amino acid residues mutated in the second motif are involved in substrate (cAMP) or inhibitor (cGMP) binding. Amino acid residues N845, E866, E971, F972, and F1004 are involved in cAMP binding, while Y751, H836, H840, E866, D950, and F1004 are involved in cGMP binding. E866 and F1004 are of special interest because they appear to be involved in both cAMP and cGMP binding. The results of protection studies are consistent with the data from site-directed mutagenesis (4, 21) and the data from chemical modification (10), suggesting an overlap of the cAMP and cGMP binding regions in the active site of PDE3A.

Both  $S_p$ -cAMPS-(BDB) and  $S_p$ -8-BDB-TcAMPSMe have proven to be effective active site-directed irreversible cAMP affinity labels for platelet PDE3A. Since the reactive carbon (C10) of  $S_p$ -8-BDB-TcAMPSMe is 8.6 Å away from the reactive carbon (C9) of  $S_p$ -cAMPS-(BDB), these two compounds together can be used to identify unique amino acids in the active site of PDE3A.

## REFERENCES

1. Juilfs, D. M., Soderling, S., Burns, F., and Beavo, J. A. (1999) *Rev. Physiol. Biochem. Pharmacol.* 135, 67–104.
2. Salzman, E. W., and Weisenberger, H. (1972) *Adv. Cyclic Nucleotide Res.* 1, 231–247.
3. Cheung, P. P., Xu, H., McLaughlin, M. M., Ghazaleh, F. A., Livi, G. P., and Colman, R. W. (1996) *Blood* 88, 1321–1329.
4. Zhang, W., and Colman, R. W. (2000) *Blood* 95, 3380–3386.
5. Cheung, P. P., Yu, L., Zhang, H., and Colman, R. W. (1998) *Arch. Biochem. Biophys.* 360, 99–104.
6. Colman, R. F. (1997) *FASEB J.* 11, 217–226.
7. Colman, R. F. (1997) in *Protein Function: A Practical Approach* (Creighton, T. E., Ed.) 2nd ed., Chapter 6, pp 55–183.
8. Lee, T. T., Worby, C., Dixon, J. E., and Colman, R. F. (1997) *J. Biol. Chem.* 272, 458–465.
9. Lee, T. T., Worby, C., Bao, Z. Q., Dixon, J. E., and Colman, R. F. (1998) *Biochemistry* 37, 8481–8489.
10. Mseeh, F., Colman, R. F., and Colman, R. W. (2000) *Thromb. Res.* 98, 395–401.
11. Grant, P. G., DeCamp, D. L., Bailey, J. M., Colman, R. W., and Colman, R. F. (1990) *Biochemistry* 29, 887–894.
12. Omburo, G. A., Torphy, T. J., Scott, G., Jacobitz, S., Colman, R. F., and Colman, R. W. (1997) *Blood* 89, 1019–1026.
13. Hung, S. H., Madhusoodanan, K. S., Beres, J. A., Boyd, R. L., Baldwin, J. L., Zhang, W., Colman, R. F., and Colman, R. W. (2001) *Bioorg. Chem.* (in press).
14. Colman, R. F. (1990) *The Enzymes* (Sigman, D. S., and Boyer, P. D., Eds.) 3rd ed., Vol. 19, pp 293–321, Academic Press, New York.
15. Lundblad, R. L., and Noyes, C. M. (1985) *Chemical reagents for protein modification*, Vol. II, Chapter 1, CRC Press, Boca Raton, FL.
16. Wrzeszczynski, K. O., and Colman, R. F. (1994) *Biochemistry* 33, 11544–11553.
17. DeCamp, D. L., Lim, S., and Colman, R. F. (1988) *Biochemistry* 27, 7651–7658.
18. Lee, P., Gorrell, A., Fromm, H. J., and Colman, R. F. (1999) *Arch. Biochem. Biophys.* 372, 205–213.
19. Colman, R. F., Huang, Y. C., King, M. M., and Erb, M. (1984) *Biochemistry* 23, 3281–3286.
20. Grant, P. G., and Colman, R. W. (1984) *Biochemistry* 23, 1801–1807.
21. Zhang, W., Ke, H., Tretiakova, A. P., Jameson, B., and Colman, R. W. (2001) *Protein Sci.* 10, 1481–1489.

22. Xu, R. X., Hassell, A. M., Vanderwall, D., Lambert, M. H., Holmes, W. D., Luther, M. A., Rocque, W. J., Milburn, M. V., Zhao, Y., Ke, H., and Nolte, R. T. (2000) *Science* 288, 1822–1825.
23. Eckstein, F., and Goody, R. S. (1976) *Biochemistry* 15, 1685–1691.
24. Jaffe, E. K., and Cohn, M. (1978) *Biochemistry* 17, 652–657.
25. Connolly, B. A., and Eckstein, F. (1982) *Biochemistry* 21, 6158–6167.
26. Park, I., Ozturk, D. H., Soundar, S., and Colman, R. F. (1993) *Arch. Biochem. Biophys.* 303, 483–488.

BI0119823